Impedance Tomography of Aplysia Abdominal Ganglion Using Multichannel Microelectrode Arrays

H. Elmariah, K. Dockendorf, S. Zhang, R. Sadleir, and T. B. DeMarse
Department of Biomedical Engineering, University of Florida, Gainesville, Florida, USA
e-mail: elmariah@ufl.edu, karld@ufl.edu, zsunguk@ufl.edu, sadleir@ufl.edu, tdemarse@ufl.edu

Abstract - **For years, researchers have studied impedance changes in neural tissue resulting from increased neuronal activity. Here, we explore this relationship using voltages recorded on a 60-channel micro-electrode array. Specifically, we show that increased action potential firing events (spikes) produced changes in the average impedance of the tissue. In each trial, changes in the amplitude of a sinusoidal carrier wave caused by an injected subthreshold current were analyzed in order to determine these impedance changes. Higher frequency data, obtained after the carrier wave was removed, were analyzed to determine the location and frequency of spike events. We here validate the utility of the 60-channel micro-electrode array for this purpose and outline future, more detailed experiments.**

Keywords - **impedance, micro-electrode array, *Aplysia*, neuron, abdominal ganglion**

I. INTRODUCTION

One of the central problems of neuroscience is to understand how information is represented and processed within the brain. It has long been recognized that the relevant unit of this representation is composed of large ensembles of neurons rather than individual neurons [1, 2]. This recognition came in part from studies of the activity of small ensembles of neurons as their behavioral correlates were simultaneously measured. Technologies such as electroencephalography (EEG), functional magnetic resonance imaging (fMRI), and multi-channel micro-electrode arrays (MEA) have enabled researchers to examine fundamental questions about the underlying dynamics of neural ensemble activity and their function within the brain.

Like any technology, each has advantages and disadvantages in terms of their spatial resolution, time resolution, or both. For example, while EEG can measure neural activity simultaneously across large areas of the cortex, it has limited spatial resolution detecting field potentials rather than individual neurons. In contrast, micro-electrode arrays can measure neural activity from both single units or field potentials from larger ensembles at relatively high sampling rates. However, its spatial resolution is limited by the density of the electrodes covering an area, which in turn is limited by the physical constraints of electrode size and the accompanying increase in hardware necessary to support such recordings. Hence, a technology that can simultaneously achieve higher resolution in both the spatial and time domains without the need for a prohibitively large number of electrodes or complex hardware would be a significant advance in this area. Rather than measuring neural activity directly through, for example, extracellular voltages, measurement of the inherent changes in conductivity that occur during neural activity offers a promising alternative that does not require an extensive network of electrodes.

Studies of conductivity changes in neural systems have been documented from as early as 1939 when Cole and Curtis demonstrated that membrane conductivity in the giant squid axon changes during the propagation of an action potential [3]. More recently, similar studies of hippocampal pyramidal cells, such as those of Fox were pursued in the 1980s [4, 5]. Generally, changes in the electrical properties (conductivity and permittivity) of biological tissue are used as an external measure that strongly reflects ion concentrations in extra- and intracellular fluids, cellular shape and density, and molecular composition, as well as membrane conductance and capacitance. At low frequencies the cell membrane is essentially non-conducting and any extra-cellular applied current will flow only in the extracellular space. Hence, intracellular conductivity will appear to be zero [6-10]. However, during activity of neural tissue there is a large increase in membrane conductance (approximately forty-fold in Cole and Curtis's studies). Thus, during activity, there is current flow through the intracellular space, which is then visible as an increase in the apparent conductivity in the intracellular region. Similarly, cortical impedance changes *in vivo* due to evoked activity and epilepsy have also been observed in cats, rabbits, and recently in humans [11-16].

In this paper, we describe an experiment to assess the feasibility of impedance as a measure of neural activity in abdominal ganglion of the invertebrate marine mollusk, *Aplysia californica,* by examining impedance changes with recordings using *in vitro* micro-electrode arrays.

II. METHOD

A. Preparation of Aplysia

Aplysia californica for these experiments were obtained from the NIH *Aplysia* Facility at the University of Miami. For each animal, a solution of 77.05 g/L of MgCl2 and 3.5745 g/L of HEPES buffer was injected into the foot process, middle, and head as a paralytic anesthetic followed by a mid-dorsal, longitudinal incision to remove the abdominal ganglion located on the posterior side of the animal near the gonopore. The abdominal ganglion contains only a few hundred cells, which are relatively large and easily visible to the naked eye [17]. Following removal, the abdominal ganglion was placed on the surface of an MEA for recording.

B. Micro-electrode Array Recordings

The neural activity of the ganglion was recorded using a 60-channel Ayanda Biosystems '3-D' MEA and the MEA1060BC system from MultiChannel Systems (sampling rate 25 kHz, bandpass 0.1-10 kHz). Platinum electrodes were arranged in an 8x8 grid and spaced 200 μm apart. Each electrode is 50 μm high with a diameter of 40 μm.

The surface of the MEA was treated with polyethyleneimine to improve adhesion of the ganglion to the recording surface of the MEA. Recordings were conducted in a bath solution containing artificial sea water (ASW) consisting of 26.8824 g/L NaCl, 0.7753 g/L KCl , 11.1815 g/L $MgCl_2$, 1.221 g/L $CaCl_2$, and 3.5745 g/L HEPES to maintain a pH of 7.8.

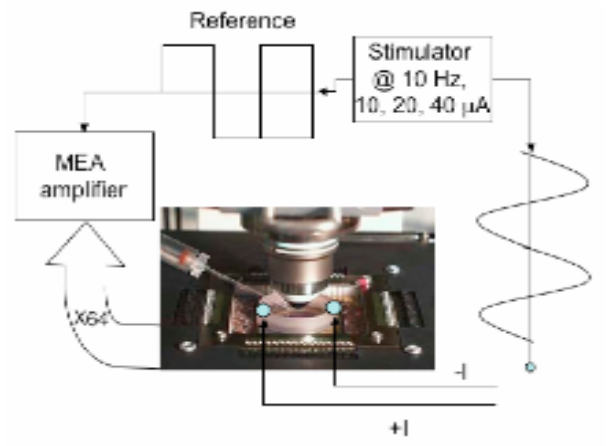

Fig. 1. Schematic representation of recording and stimulation system used to study impedance changes during neural activity of an *Aplysia* abdominal ganglion.

Approximately two minutes of baseline neural activity were recorded before impedance measurements using the external current sources began. During the impedance measurements, three 10 Hz bi-polar sine-wave currents were sequentially delivered with 10, 20, and 40 μA amplitudes, respectively. These relatively low current values were chosen to reduce the possibility of evoking activity. Current was produced by a MultiChannel Systems STG1008 8-channel programmable current and voltage stimulator. Two 2 mm diameter copper electrodes were positioned across the bath of ASW to deliver the current. Figure 1 shows a schematic representation of the recording and impedance system.

C. Filtering and Spike Detection

Application of the 10, 20, and 40 μA currents to the bath produced a significant 10 Hz frequency component during recordings whose magnitude varied according to the amplitude of the current source. The raw data during current source application was filtered using a least-mean-squares (LMS) adaptive filter [18] to remove the 10 Hz signal. Spikes were identified as voltages that were greater than five times the standard deviation of estimated noise. Figure 2 shows an example of a single spike (action potential) recorded on one channel without the 10 Hz current source, during the current source, and the corresponding output after LMS filtration of the sinusoidal signal.

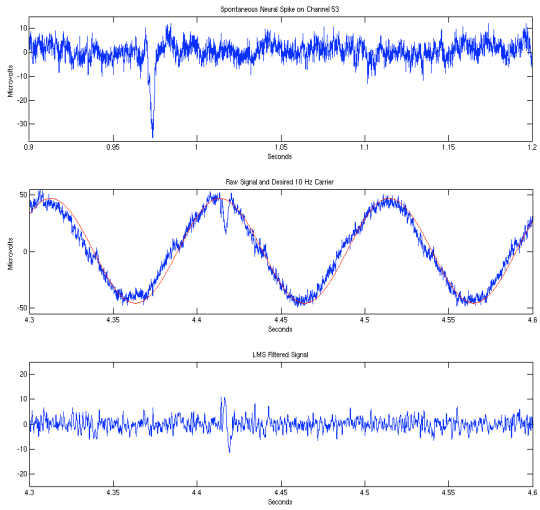

Fig. 2. Example of a spike during 1.2 seconds of baseline recordings (top), during application of the 10 μA current source (middle), and following application of the LMS filter (bottom panel).

D. Moving Average Algorithm

A moving average filter was applied to the 10, 20, and 40 μA recordings to measure any changes at frequencies near 10 Hz that occurred during neural activity. This algorithm calculated the average resistive part of the 10 Hz voltage within a sliding window of approximately 2500 samples (the period of the 10 Hz current source). Thus any changes in local conductance and impedance resulted in a change in the 10 Hz waveform, therefore effecting the moving average.

III. RESULTS

Novak et al. [19] reported differing levels of spiking activity across MEA channels that corresponded to various areas of the abdominal ganglion. Electrodes near area R15 fire continuously with bursts of activity observed every 10 seconds (0.1 Hz). Electrodes near area RB and RC would fire with irregular spike patterns at a rate of approximately 2 Hz while rostral white cells fired at rates between 0.5 and 1 Hz. We recorded similar activity patterns in our recordings. Figure 3 shows a raster plot of the spontaneous neural activity across the 60 channels observed before and after the application of the 10 μA source. Each line corresponds to a spike detected on that channel at the designated time.

During both baseline and current source recordings, spike activity on channels 8-15 (spatially clustered in the lower left quadrant of the 8x8 grid) appeared much more active relative to

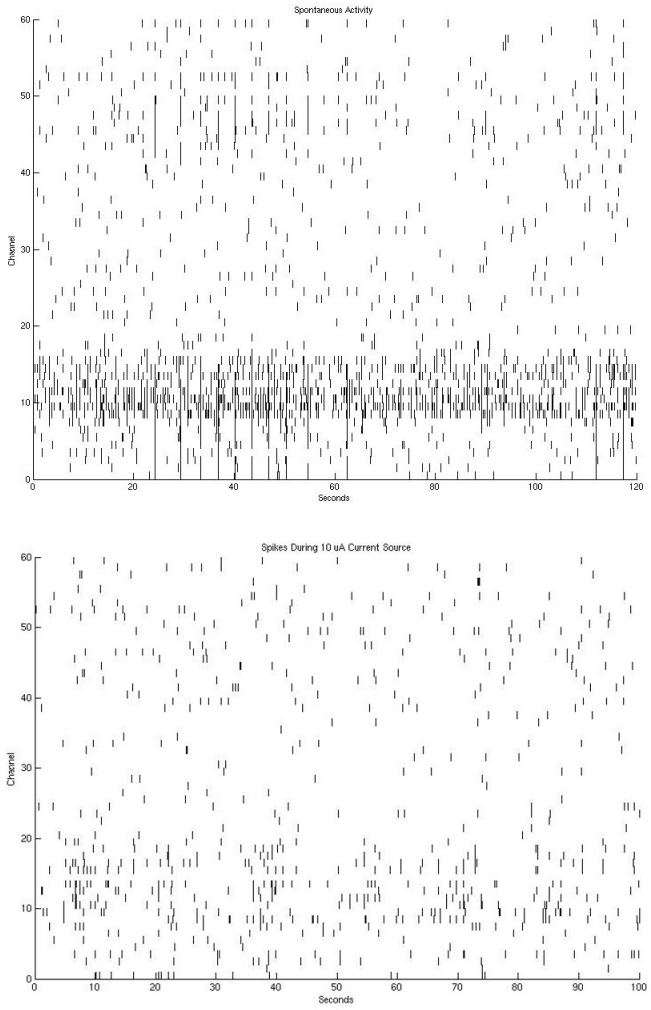

Fig. 3. Raster plot of activity over 100 seconds during baseline (top) and application of the 10 μA (bottom) current source. Each dash represents a spike event recorded on a single channel (vertical axis).

the remaining channels. Occasional bursts of activity were also observed on channels 1-7 and 42-52 occurring approximately every 10 seconds during baseline recordings. In contrast, there was little evidence for bursting during application of the current sources. These differences in activity patterns represent the different patterns produced by different cells and cell clusters located in proximity to the channels [19].

To assess the effects of spontaneous neural activity on impedance, the output of the moving average filter during the 10, 20, and 40 μA current was compared with spike timing information from the channels on the MEA. Figure 4 shows example recordings of the impedance during the presence of elevated average spike frequencies across channels for the 10 (indicated by the + symbol in Fig. 4), 20, and 40 μA recordings. Deviations in these traces indicate changes in the impedance. For example, at 170 seconds the relative impedance during each current source was modulated during the presence of spike activity. The clearest changes were recorded during the

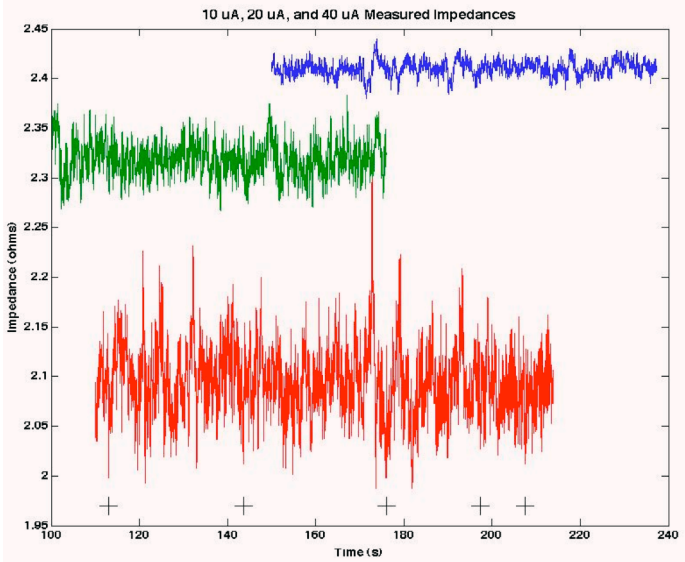

Fig. 4. Impedance during the 10, 20, and 40 μA current sources. Cross symbols represent periods of elevated spike activity for the 10 uA trace. Each trace is aligned at 170 seconds to one period of heightened activity for comparison purposes only.

40 μA current source due to the improved signal-to-noise ratio (SNR) with higher currents.

IV. DISCUSSION

Recordings from the Aplysia abdominal ganglion showed spontaneously generated activity that was consistent with prior reports using similar MEA technology [19]. Throughout the recordings, some channel clusters recorded rapid asynchronous spike activity while other areas of the array record spontaneous bursts. This pattern represents the activity of different cell types and clusters found with the abdominal ganglion of the *Aplysia*.

Application of the 10, 20, and 40 μA current sources for the impedance measurements showed modest evidence for a change in impedance during heightened spike frequencies. At the 40 μA level, changes in impedance closely followed that of changes in spike activity. However, decreasing the amplitude of the current source during the 10 μA and 20 μA trials resulted in a much poorer SNR making interpretation of that data more problematic. Perhaps an alternative analytical measure other than the moving average might reveal a stronger correlation. However, increasing the current source's amplitude also increases the possibility that the current source may eventually evoke or even synchronize the spontaneous activity patterns observed from the abdominal ganglion. For example, bursting which is clearly apparent during spontaneous baseline recordings were only marginally seen during the application of the current sources. This could be indicative of a direct influence of the current source upon the ganglion, either modifying or in some cases abolishing spontaneous burst.

Further work to improve the analytical tools to measure activity produced impedance changes may decrease the current required to reduce this effect. In addition, application of

multiple current sources (perhaps at different frequencies) may permit a more detailed analysis of activity to measure spatial localization of signals. Further tests with other tissue preparations, such as rat hippocampal slices and its inherent neural structure, will also aid in the development of this technology.

V. CONCLUSION

In summary, neural activity from the Aplysia abdominal ganglion was measured during application of three different impedance currents. Of the three currents tested, the 40 μA current produced the most promising outcome indicating modest changes in impedance relative to neural activity with reduced signal-to-noise. Improvement of our analytical tools for measuring these changes and validation through other tissue preparations, in conjunction with increased spatial resolution from multiple sources, should provide a valuable foundation for the development of impedance measurements as a tool for measuring neural activity.

ACKNOWLEDGMENT

We would like to thank Michael Furman, Alex Cadotte, and Il Park at the University of Florida for their contributions to this project.

REFERENCES

1. Georgopoulos, A.P., A.B. Schwartz, and R.E. Kettner, *Neuronal population coding of movement direction.* Science, 1986. **233**(4771): p. 1416-9.
2. Gerstner, W., et al., *Neural codes: firing rates and beyond.* Proc Natl Acad Sci U S A, 1997. **94**(24): p. 12740-1.
3. Cole, K.S. and J.C. Howard, *Electric Impedance of the Squid Giant Axon During Activity.* The Journal of General Physiology, 1939. **22**: p. 649-670.
4. Fox, S.E., *Membrane Potential and impedance changes in hippocampal pyramidal cells during theta rhythm.* Experimental Brain Research, 1989. **77**(2): p. 283-294.
5. Fox, S.E. and C.Y. Chan, *Location of membrance conductance changes by analysis of the input impedance of neurons. II. Implementation.* Journal of Neurophysiology, 1985. **54**(6): p. 1594-1606.
6. Webster, J.G., ed., *Electrical Impedance Tomography*. 1990, Bristol, UK: Adam Hilgar.
7. Holder, D., ed., *Clinical and Physiological Applications of Electrical Impedance Tomography*. 1993, London, UK: UCL Press.
8. Boone, K., D. Barber, and B. Brown, *Imaging with electricity: report of the European Concerted Action on Impedance Tomography.* J. Med Eng Technol, 1997. **21**(6): p. 201-32.
9. Grimnes, G. and O.G. Martinsen, *Bioimpedance and Bioelectricity Basics*. 2000, London, UK: Academic Press.
10. Holder, D., *Electrical Impedance Tomography of Brain Function*. 2005, London, UK: IOP Publishing.
11. Adey, W.R., R.T. Kado, and J. Didio, *Impedance measurements in brain tissue of animals using microvolt signals*. Experimental Neurology, 1962. **5**: p. 47-66.
12. Aladjolova, N.A., *Slow electrical processes in the brain.* Progress In Brain Research, 1964. **7**: p. 155-237.
13. Geddes, L. and L.E. Baker, *The specific resistance of biological material-a compendium of data for the biomedical engineer and physiologist.* Med Biol Eng, 1967. **5**(3): p. 271-93.
14. Tidswell, A.T., et al., *Electrical impedance tomography of human brain activity with a two-dimensional ring of scalp electrodes.* Physiol Meas, 2001. **22**(1): p. 167-75.
15. Ranck, J.B., Jr., *Specific impedance of rabbit cerebral cortex.* Experimental Neurology, 1963. **7**: p. 144-52.
16. Van Harreveld, A. and J.P. Schade, *Changes in the electrical conductivity of cerebral cortex during seizure activity.* Experimental Neurology, 1962. **5**: p. 383-400.
17. Frazier, W.T., et al., *Morphological and functional properties of identified neurons in the abdominal ganglion of Aplysia californica.* Journal of Neurophysiology, 1967. **30**(1288-1351).
18. Haykin, S., *Adaptive Filter Theory (4th Edition)*. 2002, Upper Saddle River, NJ: Prentice Hall.
19. Novak, J.L. and B.C. Wheeler, *Recording from the Aplysia Abdominal Ganglion with a Planar Microelectrode Array.* IEEE Transactions on Biomedical Engineering, 1986. **BME-33**(2): p. 196-202.